Journal of Cellular Physiology

Altered Bone Development and Turnover in Transgenic Mice Over-Expressing Lipocalin-2 in Bone

DELFINA COSTA,[1] EDOARDO LAZZARINI,[1] BARBARA CANCIANI,[1] ALESSANDRA GIULIANI,[2] RAFFAELE SPANÒ,[1] KATIA MAROZZI,[2] ADRIAN MANESCU,[2] RANIERI CANCEDDA,[1] AND SARA TAVELLA[1]*

[1]*Dipartimento di Medicina Sperimentale, Universita' di Genova & IRCCS AOU San MartinoIST, Istituto Nazionale per la Ricerca sul Cancro, Genova, Italy*

[2]*Dipartimento di Scienze Cliniche Specialistiche e OdontostomatologicheSezione di Scienze Fisiche, UniversitÁ Politecnica delle Marche, Ancona, Italy*

Lipocalin-2 (LCN2) is a protein largely expressed in many tissues, associated with different biological phenomena such as cellular differentiation, inflammation and cancer acting as a survival/apoptotic signal. We found that LCN2 was expressed during osteoblast differentiation and we generated transgenic (Tg) mice over-expressing LCN2 in bone. Tg mice were smaller and presented bone microarchitectural changes in both endochondral and intramembranous bones. In particular, Tg bones displayed a thinner layer of cortical bone and a decreased trabecular number. Osteoblast bone matrix deposition was reduced and osteoblast differentiation was slowed-down. Differences were also observed in the growth plate of young transgenic mice where chondrocyte displayed a more immature phenotype and a lower proliferation rate. In bone marrow cell cultures from transgenic mice, the number of osteoclast progenitors was increased whereas in vivo it was increased the number of mature osteoclasts expressing tartrate-resistant acid phosphatase (TRAP). Finally, while osteoprotegerin (OPG) levels remained unchanged, the expression of the conventional receptor activator of nuclear factor-κB ligand (RANKL) and of the IL-6 was enhanced in Tg mice. In conclusion, we found that LCN2 plays a role in bone development and turnover having both a negative effect on bone formation, by affecting growth plate development and interfering with osteoblast differentiation, and a positive effect on bone resorption by enhancing osteoclast compartment.

J. Cell. Physiol. 228: 2210–2221, 2013.

During skeletal growth the cartilaginous growth plate is responsible of long bone growth and alteration in chondrocyte proliferation and/or differentiation (characterized by sequential expression of collagen type II and type X) leads to several skeletal malformations (Cancedda et al., 2000; Mackie et al., 2011; Zankl et al. 2005). When the animal reaches the sexual maturity the growth plate disappears and the bone stops to grow. Nevertheless, throughout the adult life, in order to maintain its strength and proper functionality, the bone is continuously remodeled (bone turnover). Bone remodeling is a tightly regulated process occurring and depending on the activity of two major cell players: bone-depositing osteoblasts of mesenchymal origin and bone-resorbing osteoclasts derived from the hematopoietic lineage.

Several molecules influence osteoblast differentiation. Among them, the transcription factors, runt-related transcription factor 2 (Runx2) is one of the main master genes involved. While the differentiation proceeds different proteins are secreted such as collagen type I, the major component of bone matrix, alkaline phosphatase (ALP), important in stabilizing the matrix, osteocalcin (OC), a non-collagenous protein almost exclusively expressed in bone and up-regulated at late osteoblast differentiation stages at the time of the mineralization onset (Mackie, 2003).

Osteoblasts influence osteoclast differentiation through the expression of RANKL, that links to its receptor, RANK, present on the surface of pre-osteoclasts, whose differentiation includes the expression genes important for their bone resorbing activity such as the tartrate-resistant acid phosphatase (TRAP) (Kollet et al., 2007). Osteoprotegerin (OPG), functioning as a soluble decoy receptor for RANKL, antagonizes the RANKL positive effects on osteoclasts. OPG and RANKL act as a key molecular axis for osteoclast formation, function, and survival and provide a crucial regulation of bone remodeling and bone mass (Simonet et al., 1997).

Other factors, such as TNF-α, IL-1, IL-6, parathyroid hormone, vitamin D3, and prostaglandins are known to promote osteoclast formation (Azuma et al., 2000).

Delfina Costa and Edoardo Lazzarini contributed equally to this work.

Contract grant sponsor: Italian MIUR.
Contract grant sponsor: Italian Space Agency (ASI).

*Correspondence to: Sara Tavella, Lab. Medicina Rigenerativa, Dipartimento di Medicina Sperimentale, c/o CBA, Università di Genova, Largo Rosanna Benzi 10, 16132 Genova, Italy.
E-mail: sara.tavella@unige.it

Manuscript Received 13 August 2012
Manuscript Accepted 10 April 2013

Accepted manuscript online in Wiley Online Library (wileyonlinelibrary.com): 20 April 2013.
DOI: 10.1002/jcp.24391

Among them, IL6 is a pleiotropic cytokine playing an important role in the inflammatory response and known for its capacity to simultaneously generate functionally distinct and sometimes contradictory signals, depending on the environment contest (Ishimi et al., 1990; Tamura et al., 1993; Heinrich et al., 2003; Kamimura et al., 2003). Indeed, IL-6 can promote osteoclast maturation and activation and, at the same time, influence bone formation (Ishimi et al., 1990; Franchimont et al., 2005; Li et al., 2008; Lorenzo et al., 2008).

In particular IL-6 and IL-11, produced by several cell types present in the bone microenvironment, can promote osteoclastogenesis and bone resorption via a signal transducer glycoprotein-130 (gp-130) (Pflanz et al., 2000; Kudo et al., 2003; Sims et al., 2004).

Lipocalin-2 (LCN2) is a member of the lipocalin family, which includes several small secreted proteins functioning as modulators of different physiological processes during both embryogenesis and adult life (Liu and Nilsen-Hamilton, 1995; Akerstrom et al., 2000; Flower et al., 2000; Kjeldsen et al., 2000; Ulivi et al., 2008). LCN2 binds iron influencing cellular proliferation rate. LCN2-KO mice displayed a higher sensibility to *Escherichia coli* infections but no other obvious phenotype (Flo et al., 2004).

During inflammation, LCN2 is variously expressed in different organs by several cell types. In bone cartilage development, LCN2 is one of the major proteins synthesized and secreted by pre-hypertrophic/hypertrophic chondrocytes. When added to cultures of the ATDC5 cell line, the protein affected chondrocyte proliferation and differentiation suggesting a role in the cartilage growth plate (Meheus et al., 1993; Liu et al., 1997; Zerega et al., 2000; Ryon et al., 2002; Nilsen-Hamilton et al., 2003; Yang et al., 2003; Owen et al., 2008; Ulivi et al., 2008). More recently, we reported that LCN2 is expressed in bone and that, in transgenic mice over-expressing LCN2 under the control of the COLIα1 promoter, it controls the expression of stromal cell-derived factor-1 (SDF-1) and the number of responsive cells in the bone marrow. Regardless of the wide characterization of its expression in several processes, LCN2 function remains unclear.

We investigated the role of LCN2 in the skeleton development and turnover taking advantage of the transgenic mice model we developed. The investigation was supported by synchrotron radiation X-ray computed microtomography (MicroCT) analysis to detect alterations of bone microarchitecture consequent to the LCN2 over-expression. In the present study we show that during osteoblast differentiation, LCN2 expression is regulated in parallel with the expression of its receptor BOCT (Brain type Organic Cation Transporter) (Richardson, 2005). Additional experiments in vitro and in vivo observations indicated LCN2 as a new player in the control of bone development and turnover. In fact, LCN2 exerts both a negative effect on bone formation by affecting growth plate development and interfering with osteoblast differentiation and a positive effect on bone resorption by increasing osteoclast maturation, likely through an enhancement of RANKL and IL-6 expression.

Materials and Methods

LCN-2 transgenic mice

The full-length cDNA of the mouse LCN2 was cloned between the *Hin*dIII and *Eco*RI site of the mouse pro alpha 1 collagen I promoter plasmid containing a Bovine polyadenylation addition site (Bpa) (Costa et al., 2010). The transgene was injected into the pronuclei of FVB mice fertilized eggs that were later implanted into CD1 pseudo-pregnant foster mothers. Transgenic (Tg) mice were identified by PCR analysis, using the *Lcn2* primers: forward 5′-ACCACGGACTACAACCAGTTCG-3′ and reverse, 5′-GGAGGGGCAAACAACAGATGG-3′ selected in the Bpa region to amplify specifically only the transgene. In addition a Southern blot analysis of *Eco*RI digested genomic DNA, hybridized with a transgene specific probe was performed (not shown).

Mice were bred and maintained at the Institution's animal facility (IST, Genova, Italy). The care and use of the animals were in compliance with laws of the Italian Ministry of Health and the guidelines of the European Community.

Cell cultures

Wild-type (Wt) and transgenic (Tg) osteoblasts were obtained for each culture condition from at least three independent cell primary cultures starting from pools of calvaria of four mice each. Briefly, calvaria from newborn mice were isolated, cleaned, and chopped. Bone chips were then digested with sequential solutions of collagenase I (0.6 mg/ml), and trypsin (0.5 mg/ml) in Ringer's solution for 15, 20, and 30 min. Supernatants were discarded and the pellets were processed with two additional successive 50 and 60 min digestions in collagenase I. The obtained cells were washed, suspended in DMEM medium with 10% FBS and plated in culture dishes. Confluent primary cells (T0) cultured with DMEM 10% FBS, were stimulated with ascorbic acid 50 mg/ml, beta-glycerophosphate 10 mM, dexamethasone (DEX) 10^{-7} M (T0) to obtain osteoblast differentiation. Differentiation was evaluated after 3 (T3) and 5 (T5) weeks of culture.

Murine osteoblast cell line MC3T3-E1 was cultured in the presence of an LCN2 enriched fraction from the FPLC purification of tg osteoblast conditioned medium (Costa, 2010 #1). After 22 h, cells were collected and processed for quantitative PCR analysis as described below.

Western blot analysis

Western blot for LCN2 detection was performed with serum free conditioned media of osteoblasts and with BM lysates. Equal amount of total proteins, measured by Bradford assay, were loaded on a 12% reducing SDS–PAGE. After electrophoresis, the gel was blotted to a BA85 nitrocellulose membrane (Schleicher and Schuell GmbH, Dassel, Germany) according to the procedure described by Towbin et al. (1979). The blot was saturated for 16 h with 5% non-fat cow milk in TTBS buffer and incubated over night at 4°C with the anti-rabbit LCN2 (kindly provided by Dr. M. Nilsen-Hamilton). After washing, the detection was performed by a conjugated HRP-anti-rabbit IgG (GE Healthcare Bio-Sciences, Piscataway, NJ) using the ECL Western blotting detection reagents (GE Healthcare Bio-Sciences, Piscataway, NJ).

Image acquisition, image reconstruction, and data analysis protocol

Tg and Wt femurs of 2-, 5-, and 12-month-old mice (six animals per group) were analyzed. The X-Ray MicroCT acquisition was performed at the SYRMEP Beamline of the ELETTRA Synchrotron Radiation Facility, Trieste, Italy. The experiments were conducted with beam energy of 19 keV, pixel size of 9 μm and 1,200 angular projections over 180°. After radiographic data acquisition, the 3D virtual reconstruction was performed by means of a 3D filtered back-projection algorithm to retrieve the 3D bone structure image. The investigated volumes were physically selected in the lower third of the right femurs from the patella towards the shaft of the femur.

Bone 3D microarchitecture parameters were determined by microCT in the trabecular structure of a restricted sub-volume, which corresponded to a rectangular prism, $\sim$3,800 μm high for 2-month-old mice and $\sim$4,700 μm high for 5- and 12-month-old mice and with a base taken as the largest area fully included in the trabecular structure and excluding cortical bone. The different ROI height between 2-month old and the other mice is due to the need to consider always the same anatomical portion

independently to the growing stage. The trabecular structure inside the femur was imaged in three dimensions to obtain 3D quantitative parameters of trabecular bone architecture by the VG Studio Max commercial software (Hildebrand and Ruegsegger, 1997). The quantification of trabecular structures is based on parameters obtained from the 3D trabecular bone images. The measurement method includes direct computation using a plate-model assumption (Parfitt et al., 1983; Kuhn et al., 1990) in the three-dimensional analysis. We used this approach to compute the following 3D parameters on the trabecular ROIs: total volume (TV—expressed in μm^3), bone volume (BV—expressed in μm^3), bone volume to total volume ratio (BV/TV—expressed as a percentage), bone surface to bone volume ratio (BS/BV—per millimeter), trabecular thickness (TbTh—expressed in micrometers), trabecular number (TbN—per millimeter), and trabecular separation (TbS—expressed in micrometers). We also compared the thickness distributions of the trabecular structures between Tg mice and the respective Wt controls.

In the case of cortical analysis, a 540 μm thick portion, 4 mm for 2-month old and 5.5 mm for the other 5- and 12-month-old mice, far away from the patella was considered.

Real-time RT-PCR analysis

Total RNA was extracted from primary culture of OB from calvariae, entire femur, BM flushed from femur and whole grinded femurs, of Wt and Tg mice of different ages. Briefly, samples were homogenized in Tryzol and RNA was obtained according to the manufacture's protocol (Sigma Aldrich, St. Louis, MO) with a final purification with LiCl. Total RNA was digested with DNAse in order to eliminate possible contamination of genomic DNA. Different mRNA levels were measured by semiquantitative or real-time quantitative RT-PCR using the PE ABI PRISM 7700 Sequence Detection System (Applied Biosystems, Foster City, CA). Expression of the housekeeping gene glyceraldehyde-3-phosphate dehydrogenase (GAPDH) was measured in parallel as endogenous control. The sequences of forward and reverse primers were designed using the Primer Express 1.5 software (Applied Biosystems) as follows: *Gapdh*: forward 5′-TGTGTCCGTCG-TGGATCTG-3′, reverse 5′-GATGCCTGCTTCACCACCTT-3′, *Trap*: forward 5′-CTACCTGTGTGGACATGACCA-3′, reverse 5′-GCACATAGCCCACACCGTTC-3′, *Rankl*: forward 5′-GTGGTCTGCAGCATCGCT-3′, reverse 5′-CACTCTC-CAGAGTCGAGTC-3′, *Sclerostin*: forward 5′-TGTCAGGAAG-CGGGTGTAGTG-3′, reverse, 5′-TCCTCCTGAGAACA-ACCAGAC-3′, *Col1*: forward 5′-GACCTGGGTGAGGCTGGT-3′, reverse 5′-CAGTATCACCAGGTTCACC-3′, *Col10*: forward 5′-TGCTGCTAATGTTCTTGACCC-3′, reverse 5′-GGAATG-CCTTGTTCTCCTCTTA-3′, *Osteocalcin*: forward 5′-CAGCG-GCCCTGAGTCTGA-3′, reverse 5′-CCTCCTGCTTGGAC-ATGAA-3′, *Alp*: forward 5′-GGACATCGCATATCAGCTAAT-3′, reverse 5′-GTATCCCACATCAGTTCTGTTC-3′, *Runx2*: forward 5′-GCACTGGCGGTGCAACAAG-3′, *Boct*: forward 5′-GAACGATGCTGGCATCACAAC-3′ reverse 5′-GTCTCTG-GCAACAGCAGATG-3′, *Lcn2*: forward 5′-GGGCAGGTGG-TACGTTCT-3′, reverse 5′-TCGTAAAGCTGCCTTCTGT-TTTT-3′.

All oligos were located at the junction between two exons. Relative transcript levels were determined from the relative standard curve constructed from stock cDNA dilutions, and divided by the target quantity of the calibrator according to the manufacturer's instructions.

ELISA assay

Concentration of IL-6 was measured in BM supernatant, serum from 2-month-old mice and in serum free conditioned media from osteoblasts culture, using mouse IL-6 ELISA (R&D System, Minneapolis, MN), according to the manufacture instructions. BM supernatants were obtained from femurs of a pool of at least three mice. Bones were flushed with 500 μl of PBS. After centrifugation, an equal amount of total proteins, measured by Bradford assay, was utilized to determine IL-6 concentrations.

The ELISA assay on the conditioned media by both Wt and Tg osteoblasts were performed from at least three independent primary cultures.

Histology

After mice sacrifice, femurs, tibiae, vertebral column, and calvariae from Tg and Wt mice were collected from neonatal, 2 weeks, 2- and 5-month-old animals.

Samples were fixed in 3.7% paraformaldehyde overnight, then washed with PBS. Some samples were decalcified in Osteodec (BioOptica, Milan, Italy), dehydrated in ethanol ascending scale grade and embedded in paraffin. Other samples were processed for resin embedding. Femurs and scaffolds processed for paraffin were cut at 5 μm thickness. Samples were stained with hematoxylin/eosin, toluidine blue stain and immunohistochemistry.

To obtain the resin embedded samples after dehydration, the calvariae, the femurs, the tibiae and the vertebral column were infiltrated with the light-curing resin Technovit 7200 VLC (Kulzer, Wehrheim, Germany) for 21 days under vacuum, changing the resin every 7 days. Samples were polymerized by the EXAKT 520 polymerizator system (EXAKT Technologies, Oklahoma City). Curing was performed at 450 nm light with the temperature of the specimens never exceeding 40°C. The specimens were then prepared to be cut, according to the precision paralleling-guide procedure protocol, using the precision presses Exakt 401 and 402 Vacuum Adhesive Press (EXAKT Technologies). Sections were then cut using the EXAKT 310 CP cutting unit (EXAKT Technologies). The sections obtained were approximately 200 μm in thickness. Sections were then grinded to 20–30 μm using the EXAKT 400 CS micro grinding unit (EXAKT Technologies). Sections were stained with Stevenel's/Van Gieson stain. Images were taken using Axiovert 200M microscope (Carl Zeiss, Oberkochen, Germany) for general morphology and histomorphometric analysis. Measure of the growth plate thickness in 2 weeks old mice, osteoblasts surface (percent of bone surface occupied by osteoblasts), its mean thickness (given in micrometers for osteoid seams) and numbers of osteocytes per area in 2-month-old long bones mice were taken.

BrdU incorporation and immunohistochemistry

BrdU incorporation was performed by intraperitoneally injecting Wt and Tg mice with 50 mg BrdU/g of body weight 90 min before sacrifice. Samples were collected as previously described. Paraffin embedded section were hydrated through ethanol graded scale, endogenous peroxidase were blocked in methanol and 3% H_2O_2. For BrdU detection antigen retrieval was done with 2N HCl, while for ColII and ColX detection the antigen retrieval was performed by incubation with 1 mg/ml hyaluronidase in PBS pH6. Pure Goat Serum was used for blocking the aspecific sites. Primary antibodies were: monoclonal anti-BrdU 1:100 (Invitrogen, Carlsbad, CA), rabbit anti-Col-II (Millipore, Billerica, MA) and rabbit anti-Col-X 1:100 (generous gift of Dr. Lunstrum, Shriners Hospital, Portland, OR). Normal IgGs (Santa Cruz Biotechnology, Santa Cruz, CA) of the same species and at the same concentration were used as controls for each antibody and no staining was observed (not shown). Detection of immunoreactivity was revealed by 3,3′-diaminobenzidine (DAB Dako, Glostrup, Denmark). To analyze the proliferation of chondrocytes in the growth plate, number of BrdU positive nuclei on the total cells was counted. In particular we considered 3 Wt and 3 Tg, we processed three sections each and we count 1,500 cells per animal.

Double calcein labeling

Four animals per group were injected intraperitoneally with calcein (10 mg/kg; Sigma-Aldrich) double time at interval of 9 days, the mice were sacrificed 4 days after the last injection. Femurs and calvariae were processed for resin embedding as previously described. Images of unstained sections were taken at wavelength of 510 nm by fluorescent microscope. Femural trabeculae, diaphysial femur, and calvaria images were chosen randomly for analysis. Bone deposition rate was measured as the distance between double fluorescent lines. We analyzed independently the bone zone described above for each animal. We calculated the absolute numbers of events occurred in each defined calcein fluorescence thickness interval found in the bones of Wt and Tg mice. At least in 4 mice for each condition, 3 slides/samples and at least 20 fields/slide at 40× magnification were taken. A sample of analyzed image is shown in Figure 6B.

TRAP staining of bone marrow osteoclast precursors and bone samples

Total bone marrow obtained from 2-month-old Wt and Tg mice were cultured (5×10^5 cells in a 24-well plastic plate, Corning Costar, Corning, NY) in DMEM with 5% FBS, 20 ng/ml M-CSF (Sigma-Aldrich) and 2 ng/ml of soluble RANKL (LiStarFish S.r.l. Milano, Italia) for 10 days. After 10 days of culture, the osteoclast precursors were stained for TRAP activity (Sigma-Aldrich) according to the manufacturer's instructions and TRAP-positive multinucleated cells (MNCs) were counted. Sections from resin embedded samples of femurs, calvaria, and vertebral column were also stained for TRAP activity and the images were acquired using Axiovert 200M microscope (Zeiss).

Statistical analysis

Statistical significance of differences observed during ELISA, quantitative RT-PCR, cell counts, and histomorphometric analysis were assessed by two-tailed *t*-test.

Statistical significance for MicroCT analyses was performed by using Sigma Stat 3.5 software (Systat Software, San Jose, CA). Statistical significance of all quantifications was assessed by two-way analysis of variance (Blottner et al., 2009, #87) tests (also called two-factor analysis of variance). These tests measure the effects of the two factors simultaneously, namely "Factor A = mouse line (Wt or Tg)" and "Factor B = mouse age (2-, 5-, or 12-month old)". Two-way ANOVA was chosen because it is not only able to assess both factors in the same test, but also to assess whether there is an interaction between the same factors. A two-way test generates three *P*-values, one for each factor independently, and one measuring the interaction between the factors. The Holm–Sidak method was preferred among multiple comparison tests because it is considered one of the most conservative. *P* values < 0.05 were considered significant.

Results

The expression of both Lcn2 and Boct (LCN2 receptor) increases during osteoblast in vitro differentiation

We previously showed that LCN-2 is expressed in bone tissue (Costa et al., 2010). To investigate whether osteoblasts of wt mice express the Lcn2 gene, we performed semi-quantitative RT-PCR and Western blot analyses. Both Lcn2 mRNA and protein expression were negligible in undifferentiated cells (T0) and reached the highest level after 5 weeks of stimulation with osteogenic factors (T5) (Fig. 1A,B). At the end of the 5-week culture, the cells were fully differentiated as demonstrated by a positive staining with Alizarin Red assay (not shown) and by the increased level of OC mRNA expression with respect to the T0 cells (Fig. 1A). Moreover, the receptor Boct exhibited an expression pattern similar to that of its ligand, Lcn2, increasing with cell differentiation, although the Boct mRNA was already detectable in T0 osteoblast cell culture indicating therefore a potential responsiveness by these cells to LCN2 stimuli (Fig. 1A).

Both Lcn2 mRNA and protein were also detected in vivo in total BM along with the receptor Boct (Fig. 1C,D).

The LCN2-Tg mice are smaller compared with Wt

To investigate the role of LCN-2 in bone we used a transgenic mouse models over-expressing LCN-2 under the control of the mouse pro alpha 1 collagen I promoter, which was previously generated in our laboratory (Costa et al., 2010). Starting from three weeks after birth, at a gross visual examination, the transgenic mice over-expressing LCN2 appeared smaller than the Wt mice of the same age. However, radiographic analysis of the whole skeleton suggested that in Tg mice a proper skeleton proportion among the different bones was maintained (Fig. 1E).

The comparison of the growth curves for Wt and Tg mice showed that at all post-natal ages Tg mice weighted about 1.5-fold less than Wt mice (Fig. 1F). Femur length of LCN2-Tg mice was shorter than wild-type starting from 3 weeks after birth and following the animal growth curve trend (Fig. 1G).

Reduced trabecular number and bone mass in LCN2-Tg bones

To explore more in detail the bone tissue organization in Wt and Tg mice, we performed a microarchitecture analysis by microCT. The investigated volumes were selected in the lower third of the right femurs from the patella towards the shaft of the femur (Fig. 2A). In Tables 1–3 we report the mean values and the standard deviations of the main bone microarchitecture parameters measured in 2-, 5-, and 12-month-old Wt and Tg mice (six femurs per group). In the 2-month-old (Table 1) Tg mice both the total volume (TV) and the bone volume (BV) were reduced when compared with Wt mice (TV: $t = 3.853$, $P = 0.001$; BV: $t = 2.608$, $P = 0.015$), with no significant differences in the other morphometric parameters. In the 5-month-old Tg mice, the same parameters, namely the total volume (TV) and the bone volume (BV), were dramatically reduced when compared with Wt mice (Table 2) (TV: $t = 7.265$, $P < 0.001$; BV: $t = 9.287$, $P < 0.001$), resulting in a bone volume to total volume ratio (BV/TV) for Tg mice half reduced respect to Wt (BV/TV: $t = 4.079$, $P < 0.001$). The BV reduction in Tg mice was due to a significant decrease in the number of the trabeculae (TbN: $t = 3.295$, $P = 0.003$) whereas, in Wt and Tg mice, the specific surface of the trabecular structure (BS/BV) and the mean of the trabecular thickness were essentially similar. In the 1-year-old mice (Table 3), differences between Tg and Wt were less pronounced, but still with the total volume (TV) and the bone volume (BV) of the LCN2-Tg mice significantly reduced compared with Wt mice (TV: $t = 4.679$, $P < 0.001$; BV: $t = 2.957$, $P = 0.006$). The analysis of the mean trabecular thickness correlated to the animal aging revealed, limitedly to Wt mice, a significant increase from 2 to 5 months old (TbTh: $t = 3.270$, $P = 0.003$), whereas from 5 to 12 months old it decreased even if in a not significant way. Additional evidences and information are given in the histogram reporting the trabecular thickness distribution (Fig. 2B) and in the color maps of trabecular thickness distribution for 2-month-old Wt (Fig. 2C1) and Tg (Fig. 2D1) mice, 5-month-old Wt (Fig. 2C2) and Tg (Fig. 2D2) mice, and 12-month-old Wt (Fig. 2C3) and Tg (Fig. 2D3) mice. Indeed, accordingly with the mean ± SEM values reported in Tables 1–3, the color maps reveal that the reduced BV in Tg bones is due to the minor trabecular number in the same Tg bones at each age-point.

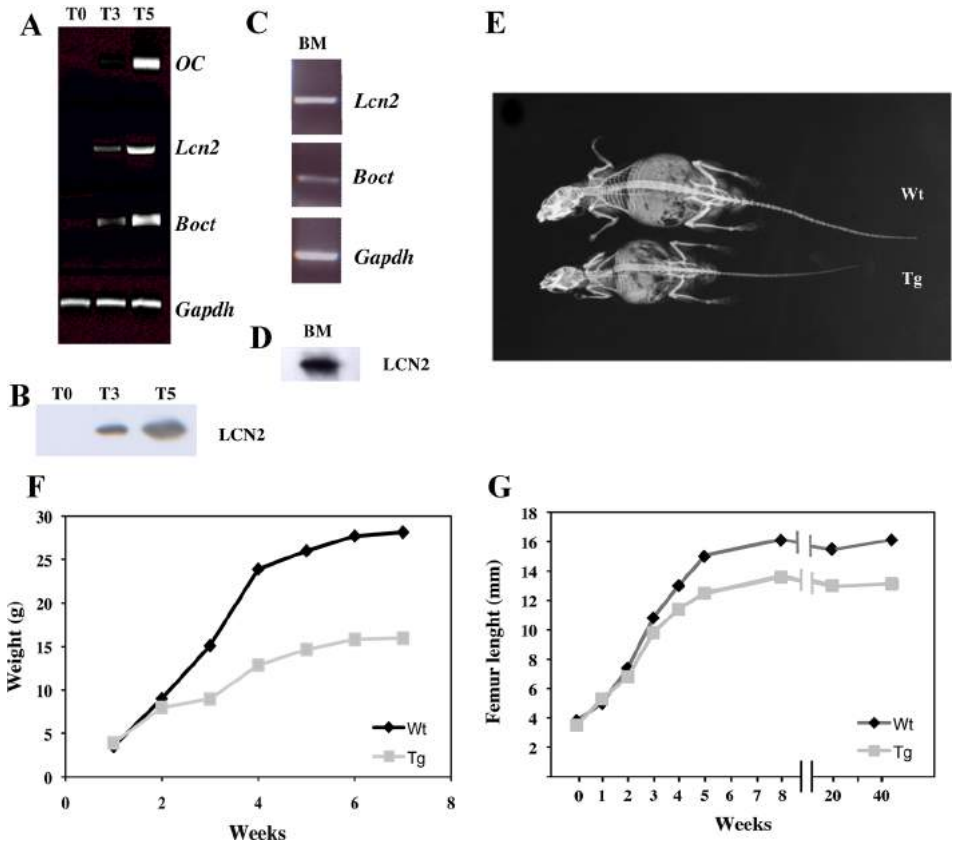

Fig. 1. Expression of LCN2 and LCN2R in bone and Wt and LCN2 transgenic mice phenotypic characterization. A: Representative figure of semiquantitative RT-PCR of RNA from osteoblast cell cultures obtained from calvaria of young mice. Cells were harvested from confluent cell culture (T0), after 3 weeks (T3) and 5 weeks (T5) of stimulation towards osteoblast differentiation. Specific primers for Lcn2 and its receptor, Boct, and osteocalcin (OC) were used. Gapdh primers were used to normalize the PCR reaction. B: Representative figure of Western blot using a polyclonal antibody anti LCN2 on T0, T3, T5 cell culture media. In the three lanes an equal amount of total proteins was loaded. C: Representative figure of RT-PCR of RNA from total BM. Specific primers for LCN2 and its receptor were used. Gapdh primers were used to normalize the PCR reaction. D: Representative figure of Western blot using a polyclonal antibody anti LCN2 on BM lysate. E: X-ray radiography image of one Wt (upper level) and one Tg (lower level) 6-month-old mouse. F: growth curve (3 animals/group) showing a reduced body weight starting at 2- to 3-week old in Tg when compared to Wt mice. G: femoral bone length between Wt and Tg mice.

By means of similar color maps, the microCT analysis confirmed the reduced cortical thickness in Tg mice compared with Wt (Fig. 3A). Evidences of this result are also supplied by the box plot graph (Fig. 3B) and the histogram of the cortical bone thickness (Fig. 3C) of the same bones.

Histological analysis confirm structural alterations in LCN2-Tg bones

To further define bone morphological changes occurring in Tg mice, we performed a histological analysis of resin embedded bones developing through both intramembranous and endochondral ossification processes. The adopted SVG stain highlights the mineralized bone tissue as a strong pink stained area whereas soft tissues are shown as blue regions. A reduced thickness of the mineralized bone was observed in the calvaria (Fig. S1A–D), as well as in longitudinal and in transversal tibial and femoral sections of Tg mice compared with Wt (Fig. S1E–H).

LCN2-Tg mice display growth plate alterations

LCN2 is already expressed during development in the cartilaginous anlagen of long bones of rats and mice (Zerega et al., 2000; Owen et al., 2008). Alteration in the cartilage growth plate organization of the transgenic animals during bone growth could very well explain the observed reduced dimension of the bones.

Indeed, histological staining of neonatal and 2-week-old mice sections revealed that the proliferating and to a higher extent the hypertrophic chondrocyte zone were less organized in Tg than in Wt mice (Figs. 4A,B and 5A,B). To investigate the differentiation pathway of chondrocytes, we performed immunohistochemical staining with collagen antibodies. In particular we obtained a higher intensity staining for type II collagen in the whole femur of Tg mice and a reduced staining for type X collagen. These results pointed to an impairment of chondrocyte maturation in transgenic mice compared with controls (Fig. 4C–F) ($n = 4$ neonatal mice). While the type II collagen mRNA level did not show a significant statistical deviation by real-time PCR between Wt and Tg mice, the type X collagen mRNA amount was reduced in tg when compared with Wt mice (Fig. 4M).

Moreover, femur growth plate measures indicated that although in the transgenic mice the hypertrophic region was shorter than in the Wt mice, a normal ratio between the hypertrophic region length and total length was maintained (Table 4).

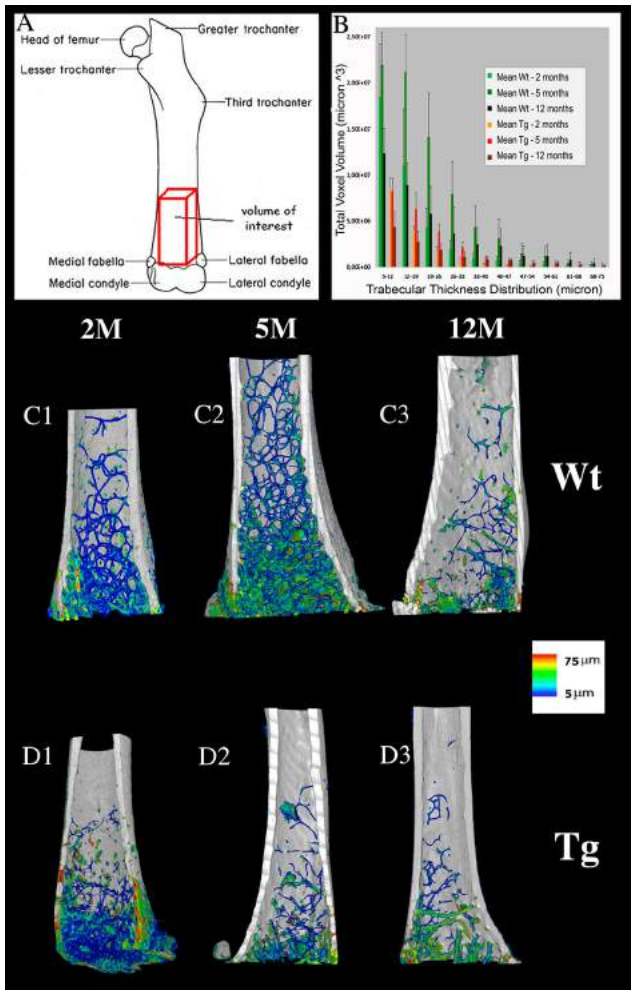

Fig. 2. Bone trabecular thickness distribution. A: Sampling volume selected for the microCT analysis. The ROI was located at ~3,800 μm high from the medial and lateral fabella for 2-month-old mice and ~4,700 μm high for the remaining 5- and 12-month-old mice. B: Quantification of trabecular thickness distribution calculated in six animals/group. Groups were Wt and Tg mice at 2-, 5-, and 12-month old. C,D: 3D color map of trabecular thickness distribution of one representative right femur of Wt (C1) and Tg (D1) of 2-month-old mice, of Wt (C2) and Tg (D2) of 5-month-old mice and of Wt (C3) and Tg (D3) 12-month-old mice.

Finally by BrdU injection analysis, we determined that in these young mice the percentage of dividing chondrocytes in the growth plate proliferating zone was reduced in Tg mice when compared with controls ($P < 0.05$) (Fig. 5C,D).

LCN2-Tg mice show a decreased bone formation rate

To investigate why in LCN2-Tg the bone mass was reduced, we analyzed the mineral apposition rate (MAR) in femurs of 2-week-old animals by double calcein labeling. In Figure 6A it is shown the measure of the distance between the two calcein labeling in trabeculae, in Tg compared to Wt mice. We observed a shift toward lower thickness values for trabeculae in the Tg mice compared to Wt ($n = 4$, $P < 0.05$). Similar observations were made in calvaria and in femoral diaphysial regions (data not shown). The finding of the decreased bone mass in Tg mice could be interpreted either with a lower matrix deposition rate by the transgenic osteoblasts or with a reduced number of osteoblasts in bones of transgenic mice. Measure of the osteoid thickness in the trabecular compartment of tibiae of 2-month-old mice revealed some heterogeneity within the same histological section. To reduce the hetereogeneity three sections were taken at different sample levels for each animal and were analyzed at least 20 fields/animal. A representative image of the double calcein labeling is shown in Figure 6B. Furthermore, to obtain statistically significant data, we performed the analysis on 6 different animals for each group (Tg and Wt; $n = 6$, $P < 0.05$) (Fig. 6C). To discriminate between the two hypotheses, we also determined the osteocyte number present in comparable area of different histological sections of bone diaphysis and the percentage of the bone surface on which osteoblasts were present (active bone deposition regions) in the two animal groups. In Table 5 we report quantitative data of bone deposition as well as osteoid width and osteocytes number. These data suggest that in the Tg mice, although the number and percentage of bone surface occupied by osteoblasts seemed normal, the process of osteoblast differentiation and the consequent bone matrix deposition appeared slowed down (Fig. 6D). However, the structural organization of the deposited bone, including the number of osteocytes/bone area (Table 4), was comparable in both Tg and Wt mice.

The transgene expression leads to an imbalance between early and late stages of osteoblast differentiation

Ten femurs per groups of 6-month-old Wt and Tg mice were grinded after flushing away the bone marrow. Total RNA was extracted from the grinded bones and a molecular analysis of the expression of some of the main osteoblast differentiation markers was performed by real-time PCR. We observed that the mRNA level of the early expression gene Runx2 was higher in Tg femurs. On the contrary, the mRNA level of the osteoblast differentiation markers expressed at later differentiation stages, such as ALP, COL1, OC, and SOST, was higher in the bones of Wt mice (Fig. 6D).

LCN2-Tg mice exhibit a higher bone resorption

Besides a diminished number of differentiated osteoblasts or a decreased bone deposition, a decreased bone mass could be also the result of an increased bone resorption. We first investigated the presence and localization of osteoclasts in the bones of 2-month-old Wt and Tg mice. We performed a TRAP staining on sections of a long bone (femur), a flat bone (calvaria) and the vertebral column obtained from three animals per group. As it was also showed by the microCT analysis, longitudinal sections of Tg femurs, including the epiphysis, showed a reduced size and a lower trabecular number (Fig. 7A, B). Moreover, at higher magnification the spongiosa trabeculae of Tg mice displayed a stronger TRAP staining and a reduced number of trabeculae compared to WT mice (Fig. 7C,D). In Tg femur transversal sections also the diaphyseal cortical bone appeared thinner and with a stronger TRAP staining (Fig. 7E,F). Similar observations were made in vertebral column sections (Fig. S2A–D) and in bone formed by intra-membranous ossification such as calvaria (Fig. S2E,F).

These findings suggested the presence of a higher bone resorption activity in Tg with respect to Wt mice. Histological observations of reduced trabecular number and thinner cortical bone were in line with the data of microCT analysis.

TABLE 1. Microarchitectural parameters in the femur trabecular structures in 2 months old mice

2 months	Wt	SEM	Tg	SEM
TV (μm^3)	1.681E+08	0.163E+08	0.795E+08	0.163E+08
BV (μm^3)	0.353E+08	0.056E+08	0.156E+08	0.062E+08
BS/BV (mm^{-1})	0.124	0.006	0.133	0.006
BV/TV (%)	2.240	0.301	1.980	0.301
Mean thickness (μm)	16.189	0.988	15.090	0.988
Mean number (mm^{-1})	1.394	0.157	1.321	0.157
Mean spacing (μm)	740	226	769	226

TABLE 2. Microarchitectural parameters in the femur trabecular structures in 5 months old mice

5 months	Wt	SEM	Tg	SEM
TV (μm^3)	2.413E+08	0.149E+08	0.886E+08	0.149E+08
BV (μm^3)	0.961E+08	0.056E+08	0.220E+08	0.056E+08
BS/BV (mm^{-1})	0.098	0.005	0.111	0.005
BV/TV (%)	4.017	0.275	2.433	0.275
Mean thickness (μm)	20.565	0.902	18.139	0.902
Mean number (mm^{-1})	2.029	0.143	1.363	0.143
Mean spacing (μm)	514	206	769	206

Increased osteoclastogenesis in LCN2-Tg mice

The increased TRAP expression observed by histochemistry in the bone sections of the Tg mice prompted us to check for the presence of osteoclast precursors and the expression of molecules involved in the osteoclastogenic process in the bone marrow of Wt and Tg mice.

We plated bone marrows flushed from bone of both mouse lines and stimulated the cultured cells with RANKL and MCS-F to promote osteoclast differentiation. After 10 days, we performed TRAP staining (Fig. 8 A1,A2). The number of TRAP positive cells was 1.8-fold increased in the marrow cultures of Tg mice compared to those from Wt mice (Fig. 8B).

In parallel, in the RNA derived from flushed femurs of 2-month-old Wt and Tg mice, we determined the mRNA level of the genes expressed in osteoblasts and mostly involved in the induction of the osteoclastogenic process (i.e., RANKL and OPG). RANKL expression was up-regulated in Tg mice, whereas the expression of OPG remained essentially similar in Wt and Tg mice (Fig. 8C). Regardless of the above findings, a higher expression of TRAP mRNA was observed in the bone marrow of Tg mice (Fig. 8D, $n = 5$, $P < 0.05$).

In agreement with the above findings, in Tg osteoblast primary cell cultures we observed an increased RANKL mRNA expression with respect to Wt cell cultures. Finally, the stimulation of the MC3T3 murine osteoblastic cell line with a FPLC fraction enriched for the LCN2, resulted in an increase of the RANKL mRNA level in a dose-dependent manner (Fig. 8E,F).

Another important factor playing a role in promoting bone loss and osteoclastogenesis is IL-6. We determined the IL-6 expression level in Wt and Tg cells in vivo and in vitro.

Indeed, the supernatant of the flushed bone marrow from Tg mice contained an amount of IL-6, measured by ELISA assay, about threefold higher than the bone marrow supernatant from Wt mice (mean $\pm$ SD, $n = 8$, $^*P < 0.05$) as well as in the serum of Tg mice (mean $\pm$ SD, $n = 6$, $^*P < 0.05$) (Fig. 8G). Similarly, when we measured the IL-6 secreted in the medium of primary osteoblast cultures of both mice lines we again noticed that the amount of IL-6 in the medium from Tg osteoblast cultures was threefold higher than in the medium from the Wt corresponding cultures (mean $\pm$ SD, $n = 4$, $^*P < 0.05$) (Fig. 8H).

Discussion

LCN2 is a protein widely expressed in many tissues, associated with different biological phenomena such as cellular differentiation, inflammation, and cancer and acting as a survival/apoptotic signal. In the skeleton, LCN2 is expressed in chondrocytes during endochondral ossification (Zerega et al., 2000; Owen et al., 2008) and in the bone tissue (Costa et al., 2010). Here we show that LCN-2 mRNA is up-regulated in bone marrow and during osteoblast differentiation along with its receptor.

Capulli et al. showed an up-regulation of LCN2 expression in osteoblast cultures under a simulated microgravity condition. Since microgravity is known to affect bone mass, these authors proposed for LCN2 a role in bone turnover (Capulli et al., 2009). This prompted us to investigate the possible effect of the LCN2 over-expression on bone turnover, taking the advantage of the LCN2-Tg mice model we generated previously (Costa et al., 2010).

TABLE 3. Microarchitectural parameters in the femur trabecular structures in 1-year-old mice

12 months	Wt	SEM	Tg	SEM
TV (μm^3)	2.118E+08	0.149E+08	1.087E+08	0.163E+08
BV (μm^3)	0.353E+08	0.056E+08	0.106E+08	0.062E+08
BS/BV (mm^{-1})	0.102	0.005	0.117	0.006
BV/TV (%)	1.767	0.275	1.060	0.301
Mean thickness (μm)	20.016	0.902	17.629	0.988
Mean number (mm^{-1})	0.922	0.143	0.596	0.157
Mean spacing (μm)	1,225	206	2,246	226

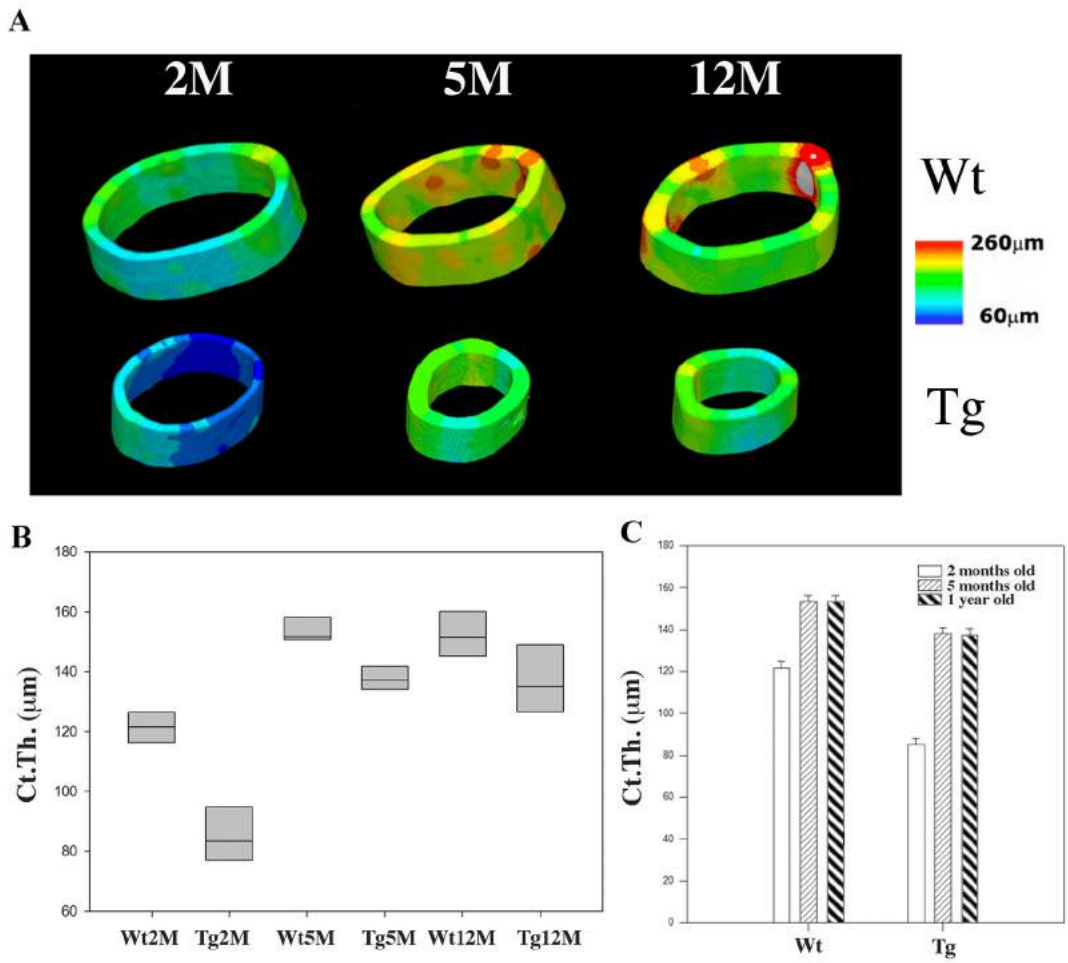

Fig. 3. Quantification of cortical thickness distribution. A: 3D color map of bone cortical thickness distribution of one representative right femur of Wt and Tg 2-, 5-, and 12-month mice. Descriptive box plots (B) and histogram (C) of the cortical thickness (CtTh[μm]).

Mice over-expressing LCN2 had a smaller skeleton compared to Wt mice of the same age, although they maintained a proper proportion among all different skeletal elements. Bones developed trough both intramembranous and endochondral ossification processes were smaller, but no major differences were observed in the bone tissue morphology and organization. The histological aspect, the osteocyte number, the osteoid width exhibited no major differences between Wt and Tg bones. Instead, a detailed microCT investigation of the bone micro-architectures evidenced that significant differences existed in the microstructure of the bone from the two mice lines. In particular, we observed that at each considered age (2, 5, and 12 months), femurs of Tg mice had a reduced cortical thickness and a reduced number of trabeculae/bone volume with respect to their Wt counterpart. Similarly, histological staining of Tg bone presented a reduced thickness and a reduced number of trabeculae. Such differences were more marked in 5-month-old mice. In Tg mice, although the number of trabeculae at 5 months of age were significantly reduced compared to Wt mice, a significant increase in trabecular and cortical thickness from 2 to 5 months combined with a significant reduction of the trabecular number parameter aging from 5-month to 1-year-old animals were observed confirming the tendency clearly evident in the Wt mice.

A possible explanation of the smaller phenotype in Tg mice could result from the observed alteration of the cartilaginous template during endochondral ossification.

Growth plate chondrocytes are fundamental for bone growth and alteration in their proliferation, differentiation, or extracellular matrix secretion can lead to several skeletal abnormalities (Shum et al., 2003; Mackie et al., 2011). In LCN2-Tg mice the chondrocytes appeared altered in their differentiation and proliferative behavior and this could, at least partially, explain the overall delay in endochondral ossification and the reduced size of the Tg mice.

A slow down of osteogenesis induced by LCN2 is also evident in the differentiation of Tg mice osteoblasts. When we compared the expression level of the main differentiation markers of the osteogenic lineage in bone from both Tg and Wt animals, we observed in Tg mice an up-regulation of the early master gene of osteoblast differentiation Runx2. On the contrary, in the same mice, gene expression of later osteoblast differentiation stage markers, such as ALP, COL1, OC, and SOST was down-regulated.

Calcein labeling experiments suggested that bones of Tg mice grew at a slower rate than Wt bones. This was confirmed by osteoid thickness measurement in histological sections although the region occupied by the osteoblasts on the bone surface remained the same in the bone of Wt mice and in the

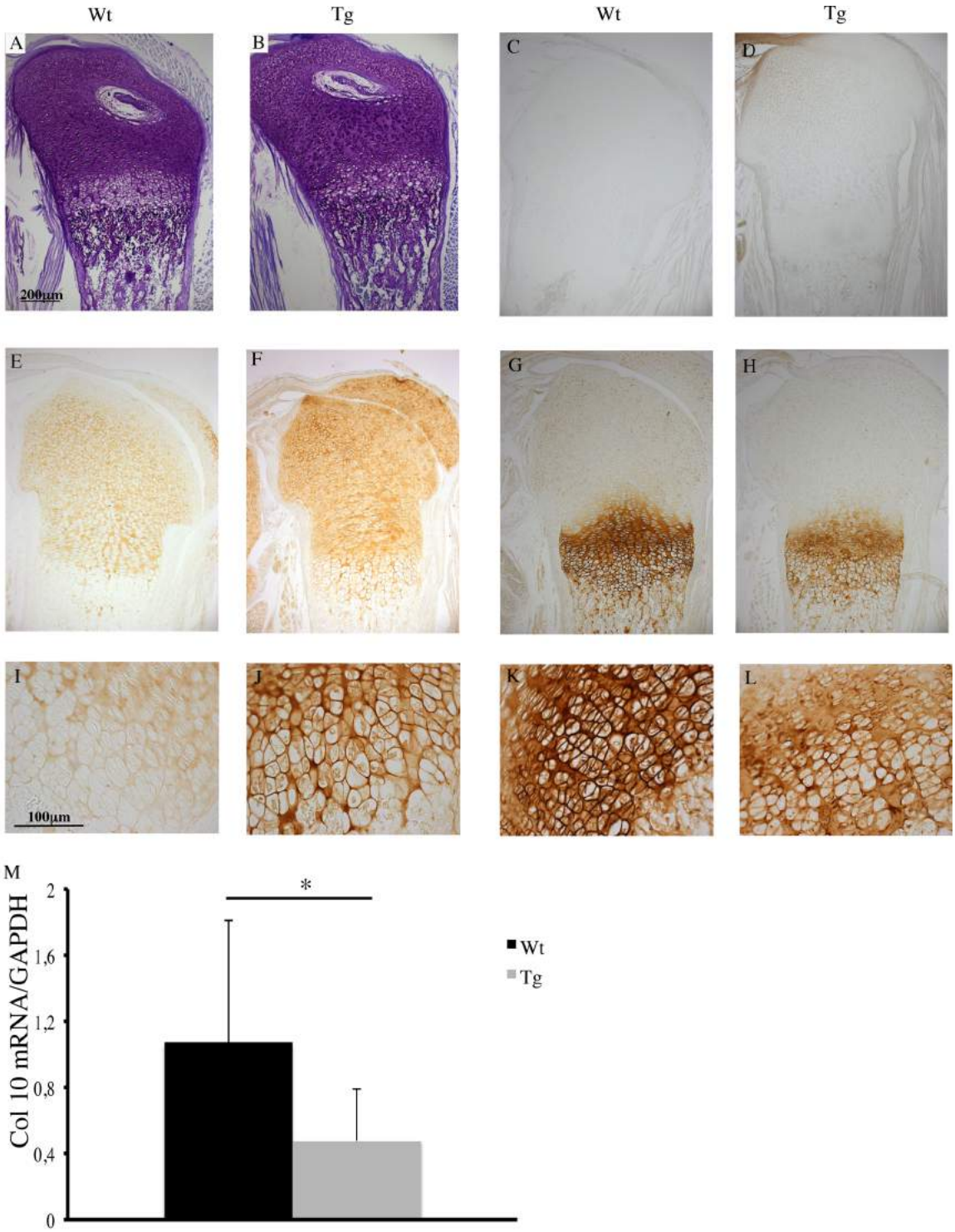

Fig. 4. Neonatal morphology in femur of Wt and Tg mice. Different organization of the growth plate in Tg (B) compared to Wt (A) by toluidine blue stain. Immunoperoxidase staining (C,D preimmune) for ColII in Wt (E) and Tg (F) showing stronger immunoreactivity in Tg mice; immunoperoxidase staining for ColX in Wt (G) and Tg (H) showing stronger immunoreactivity in Wt mice. AH images were taken at 10× magnification, IL were at 40× magnification. M: Quantification by real-time PCR of collagen 10 mRNA in neonatal bones. Data are mean ± SD, n = 8, $^{*}P < 0.05$

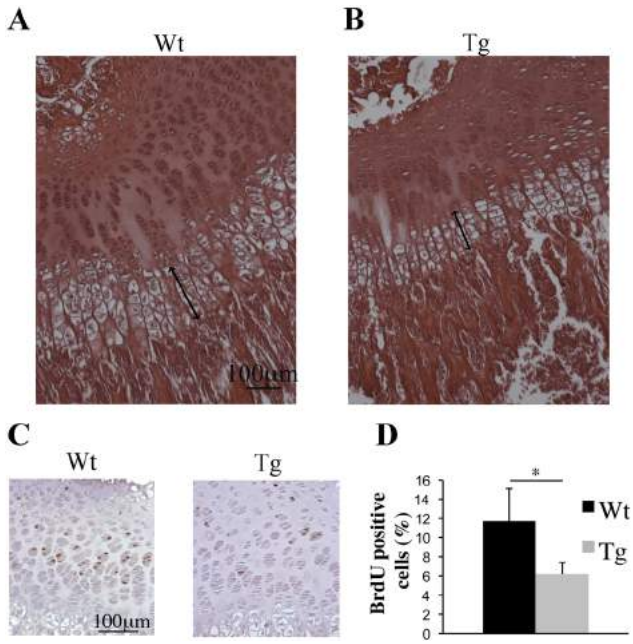

Fig. 5. Growth plate analysis in 2-week-old mice. Comparison of the hypertrophic zone thickness in Wt (A) and Tg (B) mice stained with hematoxylin/eosin stain (20× magnification). C: Images of BrdU immunoperoxidase in growth plate proliferative zone of Wt and Tg mice (40× magnification). D: Histogram showing the number of BrdU positive cells where black bars indicate Wt mice and gray bars indicate Tg mice. Data are mean ± SD, n = 3, $^*P < 0.05$.

TABLE 4. Femur growth plate histomorphometry

2 weeks	Wt	DS	Tg	DS
Total width (µm)	308	39	231	29
Hypertrophic zone width (µm)	134	17	91	13

TABLE 5. Long bone histomorphometry

2 months	Wt	DS	Tg	DS
Mineral apposition rate (µm)	10	2	7.8	1.5
Osteoblasts perimeter/bone perimeter (%)	22.89	5.9	24.49	8.7
Osteoid thickness (µm)	1.68	0.46	0.83	0.24
Osteocytes numbers/area	25	2.5	23.78	5.8

mice over-expressing LCN2, suggesting a possible similar number of osteoblasts in both mouse lines.

An increased Runx2 expression could explain, at least in part, the observed enhanced number of hematopoietic stem cells (HSC) in the Tg mice (our unpublished data). In fact, osteoblast cultures expressing high levels of Runx2 (early stages of the osteoblast lineage cell differentiation) better promote hematopoietic proliferation and function than do cultures expressing lower levels of Runx2 (more mature osteoblast lineage cells) (Chitteti et al., 2010).

A slowed down, but normal differentiation process of the osteoblasts could explain the reduced bone size observed in young and adult Tg mice and at the same time the normal organization of the formed bone tissue.

After birth bone is continuously remodeled to ensure a correct functionality of the skeleton. The reduced cortical thickness and the lower bone volume, that was demonstrated to be associated to the lower trabecular number observed in

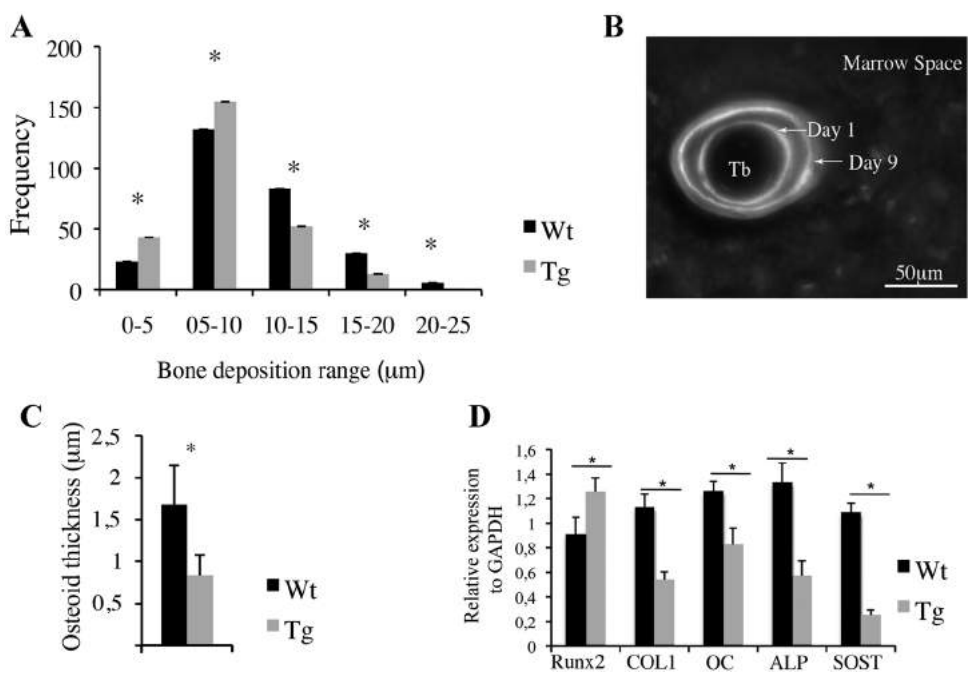

Fig. 6. AC: Bone histomorphometry in long bone of 2-month-old mice. A: Thickness distribution of double calcein labeling in femoral trabecular bone. Data are mean ± SD, n = 4, $^*P < 0.05$. B: Image of double calcein labeling in femoral trabeculae. The distance between the double fluorescent lines showed the deposition bone rate in the interval of 9 days (Tb trabecular bone, image was taken at 40× magnification). C: Osteoid thickness measured in tibial bone. Black bars indicate Wt mice and gray bars indicate Tg mice. Data are mean ± SD, n = 6, $^*P < 0.05$. D: Characterization of osteogenic lineage cells in Wt and Tg mice. A: Identification by real-time PCR of mRNA coding for different osteoblast gene markers in RNA extracted from flushed femurs of Wt (black column) and Tg (gray column). Data are mean ± SD, n = 10, $^*P < 0.05$.

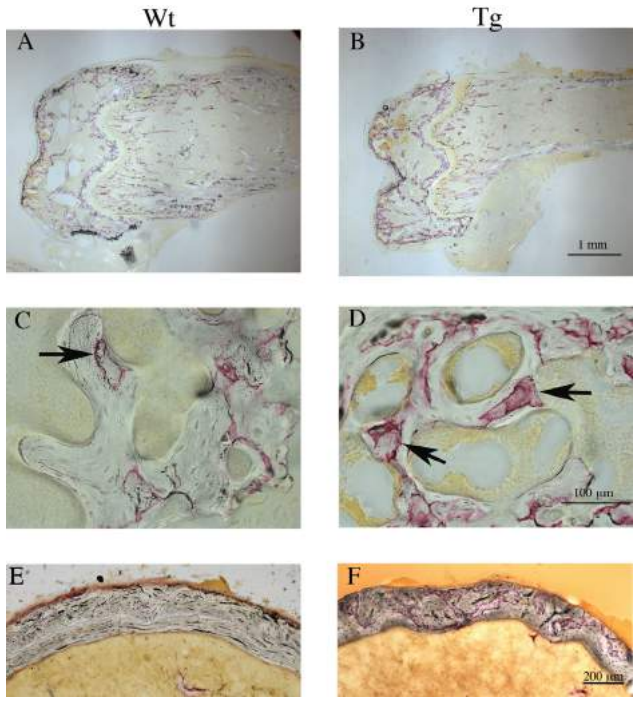

Fig. 7. TRAP expression in femurs of 2-month-old Wt and Tg mice. Left column refers to Wt mice and right column refers to Tg mice. TRAP staining of longitudinal sections of resin embedded femurs of Wt (A 2.5× and C 40× magnification) and Tg (B 2.5× and D 40× magnification) mice shows a more intense staining in Tg trabeculae compared to Wt (arrows). Also transversal sections of Tg femur diaphysis (E,F 10× magnification) show an enhanced TRAP staining.

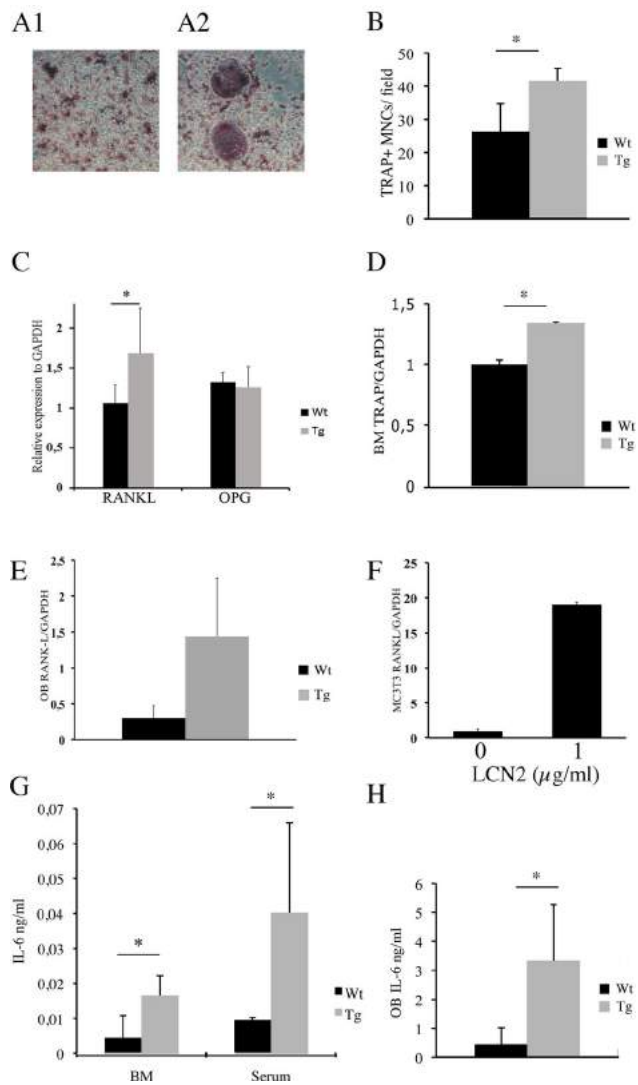

Fig. 8. In vitro TRAP staining and IL-6 expression in Wt and Tg mice. Bone marrow plated in culture dishes was supplemented with osteoclastogenic factors. After 10 days, Wt (A1) and Tg (A2) cultures were stained for TRAP (images were taken at 20× magnification). In the histograms, black bars indicate Wt mice and grey bars indicate Tg mice. B: Number of positive TRAP cells per field. C: Quantification by real-time PCR of RANKL mRNA (left) and OPG mRNA (right) in RNA extracted from flushed femurs. D: Quantification by real-time PCR of TRAP mRNA in RNA extracted from flushed bone marrow. Data are mean ± SD, n = 10, $^{*}P < 0.05$. E: Quantification by real-time PCR of RANKL mRNA in RNA extracted from Wt and Tg primary osteoblast culture cells (To). Data are mean ± SD, n = 6, $^{*}P < 0.05$. F: Quantification by real-time PCR of RANKL mRNA in RNA extracted from osteoblast MC3T3 cell line stimulated with a FPLC LCN2 enriched fraction in two different doses. Data are mean ± SD, n = 4, $^{*}P < 0.05$. G,H: Detection of IL-6 protein by Elisa in bone marrow, serum, and osteoblast conditioned media. Serum and equal amount of total proteins from the supernatant of flushed BM (G) in Wt and Tg mice, data are mean ± SD, n = 6, $^{*}P < 0.05$. H: Equal amount of total protein from conditioned medium by Wt and Tg osteoblasts were tested, data are mean ± SD, n = 4, $^{*}P < 0.05$.

Tg mice, could be explained also by an enhanced osteoclastogenesis already starting at a young animal age. In fact a higher TRAP expression was noticed in Tg bones of all animal investigated. Following this observation, we showed that LCN2 stimulated the osteoclast activation both in vivo and in vitro. Most likely the classical pathway of RANKL mediates this phenomenon, being the expression of this factor enhanced in Tg mice and induced by a LCN2 enriched HPLC fraction in vitro. It is noteworthy that the mRNA level for the decoy receptor of RANKLOPG remained unchanged. The importance of this pathway has been demonstrated in OPG knockout mice, which exhibited severe osteoporosis and in transgenic mice over-expressing OPG which developed osteopetrosis (Simonet et al., 1997; Bucay et al., 1998).

Several publications report an involvement of IL-6 in the bone remodeling process (Ishimi et al., 1990; Tamura et al., 1993). In particular, it has been described that transgenic mice over-expressing IL-6 presented a phenotype resembling that of LCN2-Tg mice. To this regard, transgenic mice over-expressing IL-6 were smaller, exhibited osteopenia with alterations in the cortical and trabecular bone microarchitecture, an increase of the osteoclast number, and also a reduction in osteoblast number and function (De Benedetti et al., 2006). Despite the alterations at tissue level, ELISA assay for bone formation (OC and P1NP) and resorption (trap5b) in serum of Wt and LCN2-Tg mice did not show modifications suggesting a local effect by LCN2 not able to alter typical bone turnover hematological parameters (data not shown).

Our data indicate thatLCN2 is a factor that negatively regulates bone matrix deposition and impairs cell lineage differentiation process to osteoblasts and osteocytes. In support to our hypothesis some papers report that, in mice in which osteoblasts over-express Runx2, the differentiation of the mesenchymal progenitors is inhibited and bone resorption is increased. This leads to the thinning of the cortices,

expansion of the marrow cavity, and possibly to spontaneous fractures (Liu et al., 2001; Geoffroy et al., 2002; Schiltz et al., 2010).

In conclusion, we propose that LCN2 is a new player in bone turnover, exerting a negative effect on bone formation and enhancing bone resorption by promoting osteoclasts maturation via RANKL andIL-6.

Acknowledgments

This work was supported by institutional funds and partially by funds from a "FIRB internazionale" grant from the Italian MIUR and from Italian Space Agency (ASI). ELETTRA User Office is kindly acknowledged for providing beam time for the micro-CT experiments. We thank Dr. Fiorella Descalzi of our institute for helpful discussions and suggestions and Dr. Giuliana Tromba, ELETTRA Synchrotron Radiation Facility, Trieste, Italy for technical support during the X-Ray microCT experiments.

Literature Cited

Akerstrom B, Flower DR, Salier JP. 2000. Lipocalins: Unity in diversity. Biochim Biophys Acta 1482:1–8.
Azuma Y, Kaji K, Katogi R, Takeshita S, Kudo A. 2000. Tumor necrosis factor-alpha induces differentiation of and bone resorption by osteoclasts. J Biol Chem 275:4858–4864.
Blottner D, Serradj N, Salanova M, Touma C, Palme R, Silva M, Aerts JM, Berckmans D, Vico L, Liu Y, Giuliani A, Rustichelli F, Cancedda R, Jamon M. 2009. Morphological, physiological and behavioural evaluation of a 'Mice in Space' housing system. J Comp Physiol B 179:519–533.
Bucay N, Sarosi I, Dunstan CR, Morony S, Tarpley J, Capparelli C, Scully S, Tan HL, Xu W, Lacey DL, Boyle WJ, Simonet WS. 1998. osteoprotegerin-deficient mice develop early onset osteoporosis and arterial calcification. Genes Dev 12:1260–1268.
Cancedda R, Castagnola P, Cancedda FD, Dozin B, Quarto R. 2000. Developmental control of chondrogenesis and osteogenesis. Int J Dev Biol 44:707–714.
Capulli M, Rufo A, Teti A, Rucci N. 2009. Global transcriptome analysis in mouse calvarial osteoblasts highlights sets of genes regulated by modeled microgravity and identifies a "mechanoresponsive osteoblast gene signature". J Cell Biochem 107:240–252.
Chitteti BR, Cheng YH, Streicher DA, Rodriguez-Rodriguez S, Carlesso N, Srour EF, Kacena MA. 2010. Osteoblast lineage cells expressing high levels of Runx2 enhance hematopoietic progenitor cell proliferation and function. J Cell Biochem 111:284–294.
Costa D, Biticchi R, Negrini S, Tasso R, Cancedda R, Descalzi F, Pennesi G, Tavella S. 2010. Lipocalin-2 controls the expression of SDF-1 and the number of responsive cells in bone. Cytokine 51:47–52.
De Benedetti F, Rucci N, Del Fattore A, Peruzzi B, Paro R, Longo M, Vivarelli M, Muratori F, Berni S, Ballanti P, Ferrari S, Teti A. 2006. Impaired skeletal development in interleukin-6-transgenic mice: A model for the impact of chronic inflammation on the growing skeletal system. Arthritis Rheum 54:3551–3563.
Flo TH, Smith KD, Sato S, Rodriguez DJ, Holmes MA, Strong RK, Akira S, Aderem A. 2004. Lipocalin 2 mediates an innate immune response to bacterial infection by sequestrating iron. Nature 432:917–921.
Flower DR, North AC, Sansom CE. 2000. The lipocalin protein family: Structural and sequence overview. Biochim Biophys Acta 1482:9–24.
Franchimont N, Wertz S, Malaise M. 2005. Interleukin-6: An osteotropic factor influencing bone formation? Bone 37:601–606.
Geoffroy V, Kneissel M, Fournier B, Boyde A, Matthias P. 2002. High bone resorption in adult aging transgenic mice overexpressing cbfa1/runx2 in cells of the osteoblastic lineage. Mol Cell Biol 22:6222–6233.
Heinrich PC, Behrmann I, Haan S, Hermanns HM, Muller-Newen G, Schaper F. 2003. Principles of interleukin (IL)-6-type cytokine signalling and its regulation. Biochem J 374:1–20.
Hildebrand T, Ruegsegger P. 1997. A new method for the model-independent assessment of thickness in three-dimensional images. J Microsc Oxford 185:67–75.
Ishimi Y, Miyaura C, Jin CH, Akatsu T, Abe E, Nakamura Y, Yamaguchi A, Yoshiki S, Matsuda T, Hirano T, Kishimoto T, Suda T. 1990. Il-6 is produced by osteoblasts and induces bone-resorption. J Immunol 145:3297–3303.
Kamimura D, Ishihara K, Hirano T. 2003. IL-6 signal transduction and its physiological roles: The signal orchestration model. Rev Physiol Biochem Pharmacol 149:1–38.
Kjeldsen L, Cowland JB, Borregaard N. 2000. Human neutrophil gelatinase-associated lipocalin and homologous proteins in rat and mouse. Biochim Biophys Acta 1482:272–283.
Kollet O, Dar A, Lapidot T. 2007. The multiple roles of osteoclasts in host defense: Bone remodeling and hematopoietic stem cell mobilization. Annu Rev Immunol 25:51–69.
Kudo O, Sabokbar A, Pocock A, Itonaga I, Fujikawa Y, Athanasou NA. 2003. Interleukin-6 and interleukin-11 support human osteoclast formation by a RANKL-independent mechanism. Bone 32:1–7.
Kuhn JL, Goldstein SA, Feldkamp LA, Goulet RW, Jesion G. 1990. Evaluation of a microcomputed tomography system to study trabecular bone structure. J Orthop Res 8:833–842.
Li Y, Backesjo CM, Haldosen LA, Lindgren U. 2008. IL-6 receptor expression and IL-6 effects change during osteoblast differentiation. Cytokine 43:165–173.
Liu Q, Nilsen-Hamilton M. 1995. Identification of a new acute phase protein. J Biol Chem 270:22565–22570.
Liu Q, Ryon J, Nilsen-Hamilton M. 1997. Uterocalin: A mouse acute phase protein expressed in the uterus around birth. Mol Reprod Dev 46:507–514.
Liu W, Toyosawa S, Furuichi T, Kanatani N, Yoshida C, Liu Y, Himeno M, Narai S, Yamaguchi A, Komori T. 2001. Overexpression of Cbfa1 in osteoblasts inhibits osteoblast maturation and causes osteopenia with multiple fractures. J Cell Biol 155:157–166.
Lorenzo J, Horowitz M, Choi Y. 2008. Osteoimmunology: Interactions of the bone and immune system. Endocr Rev 29:403–440.
Mackie EJ. 2003. Osteoblasts: Novel roles in orchestration of skeletal architecture. Int J Biochem Cell Biol 35:1301–1305.
Mackie EJ, Tatarczuch L, Mirams M. 2011. The skeleton: A multi-functional complex organ: The growth plate chondrocyte and endochondral ossification. J Endocrinol 211:109–121.
Meheus LA, Fransen LM, Raymackers JG, Blockx HA, Van Beeumen JJ, Van Bun SM, Van de Voorde A. 1993. Identification by microsequencing of lipopolysaccharide-induced proteins secreted by mouse macrophages. J Immunol 151:1535–1547.
Nilsen-Hamilton M, Liu Q, Ryon J, Bendickson L, Lepont P, Chang Q. 2003. Tissue involution and the acute phase response. Ann NY Acad Sci 995:94–108.
Owen HC, Roberts SJ, Ahmed SF, Farquharson C. 2008. Dexamethasone-induced expression of the glucocorticoid response gene lipocalin 2 in chondrocytes. Am J Physiol Endocrinol Metab 294:E1023–E1034.
Parfitt AM, Mathews CH, Villanueva AR, Kleerekoper M, Frame B, Rao DS. 1983. Relationships between surface, volume, and thickness of iliac trabecular bone in aging and in osteoporosis. Implications for the microanatomic and cellular mechanisms of bone loss. J Clin Invest 72:1396–1409.
Pflanz S, Kurth I, Grotzinger J, Heinrich PC, Muller-Newen G. 2000. Two different epitopes of the signal transducer gp130 sequentially cooperate on IL-6-induced receptor activation. J Immunol 165:7042–7049.
Richardson DR. 2005. 24p3 and its receptor: Dawn of a new iron age? Cell 123:1175–1177.
Ryon J, Bendickson L, Nilsen-Hamilton M. 2002. High expression in involuting reproductive tissues of uterocalin/24p3, a lipocalin and acute phase protein. Biochem J 367:271–277.
Schiltz C, Prouillet C, Marty C, Merciris D, Collet C, de Vernejoul MC, Geoffroy V. 2010. Bone loss induced by Runx2 over-expression in mice is blunted by osteoblastic over-expression of TIMP-1. J Cell Physiol 222:219–229.
Shum L, Coleman CM, Hatakeyama Y, Tuan RS. 2003. Morphogenesis and dysmorphogenesis of the appendicular skeleton. Birth Defects Res C Embryo Today 69:102–122.
Simonet WS, Lacey DL, Dunstan CR, Kelley M, Chang MS, Luthy R, Nguyen HQ, Wooden S, Bennett L, Boone T, Shimamoto G, DeRose M, Elliott R, Colombero A, Tan HL, Trail G, Sullivan J, Davy E, Bucay N, Renshaw-Gegg L, Hughes TM, Hill D, Pattison W, Campbell P, Sander S, Van G, Tarpley J, Derby P, Lee R, Boyle WJ. 1997. Osteoprotegerin: A novel secreted protein involved in the regulation of bone density. Cell 89:309–319.
Sims NA, Jenkins BJ, Quinn JM, Nakamura A, Glatt M, Gillespie MT, Ernst M, Martin TJ. 2004. Glycoprotein 130 regulates bone turnover and bone size by distinct downstream signaling pathways. J Clin Invest 113:379–389.
Tamura T, Udagawa N, Takahashi N, Miyaura C, Tanaka S, Yamada Y, Koishihara Y, Ohsugi Y, Kumaki K, Taga T, Kishimoto T, Suda T. 1993. Soluble interleukin-6 receptor triggers osteoclast formation by interleukin 6. Proc Natl Acad Sci USA 90:11924–11928.
Towbin H, Staehelin T, Gordon J. 1979. Electrophoretic transfer of proteins from polyacrylamide gels to nitrocellulose sheets: Procedure and some applications. Proc Natl Acad Sci USA 76:4350–4354.
Ulivi V, Cancedda R, Cancedda FD. 2008. 15-deoxy-delta 12,14-prostaglandin J (2) inhibits the synthesis of the acute phase protein SIP24 in cartilage: Involvement of COX-2 in resolution of inflammation. J Cell Physiol 217:433–441.
Yang J, Mori K, Li JY, Barasch J. 2003. Iron, lipocalin, and kidney epithelia. Am J Physiol Renal Physiol 285:F9–18.
Zankl A, Neumann L, Ignatius J, Nikkels P, Schrander-Stumpel C, Mortier G, Omran H, Wright M, Hilbert K, Bonafe L, Spranger J, Zabel B, Superti-Furga A. 2005. Dominant negative mutations in the C-propeptide of COL2A1 cause platyspondylic lethal skeletal dysplasia, torrance type, and define a novel subfamily within the type 2 collagenopathies. Am J Med Genet Part A 133A:61–67.
Zerega B, Cermelli S, Michelis B, Cancedda R, Cancedda FD. 2000. Expression of NRL/NGAL (neu-related lipocalin/neutrophil gelatinase-associated lipocalin) during mammalian embryonic development and in inflammation. Eur J Cell Biol 79:165–172.

Supporting Information

Additional supporting information can be found in the online version of this article at the publisher's web-site.

Fig. S1. Histology of bone formed by either an endochondral or an intramembranous process. Resin embedded section of two month old Wt (left column) and Tg (right column) bones were stained with Stevenel's/Van Gieson stain. Central (A,B) and lateral (C,D) portion of the calvariae, epiphysial images (E,F) of tibiae and transversal section (G,H) of femur diaphysis are presented. A–D images at 20× magnification; E,F images at 10× magnification; G,H images at 40× magnification were taken.

Fig. S2. TRAP expression in endochondral and intramembranous bones of 2-month-old Wt and Tg mice. Left column refers to Wt mice and right column refers to Tg mice. A–D show lumbar vertebrae at low (A,B 2.5×) and high (C,D 20×) magnification; E,F: middle coronal calvaria sections (20× magnification; inserts 40× magnification).